

1 Characterizing the growing microorganisms at species level in 2 46 anaerobic digesters at Danish wastewater treatment plants: 3 A six-year survey on microbiome structure and key drivers

4 Chenjing Jiang^{1,2}, Miriam Peces¹, Martin H. Andersen¹, Sergey Kucheryavskiy³, Marta
5 Nierychlo¹, Erika Yashiro¹, Kasper S. Andersen¹, Rasmus H. Kirkegaard¹, Liping Hao¹,
6 Jan Høgh⁴, Aviaja A. Hansen⁴, Morten S. Dueholm¹, Per H. Nielsen^{1*}

7 ¹Center for Microbial Communities, Department of Chemistry and Bioscience, Aalborg
8 University, Aalborg, Denmark.

9 ²Key Laboratory of Engineering Oceanography, Second Institute of Oceanography, SOA,
10 Hangzhou, China.

11 ³Department of Chemistry and Bioscience, Aalborg University, Esbjerg, Denmark.

12 ⁴Krüger Veolia, Aarhus, Denmark.

13 *Corresponding author: Prof. Per Halkjær Nielsen, Center for Microbial
14 Communities, Department of Chemistry and Bioscience, Aalborg University, Fredrik
15 Bajers Vej 7H, 9220 Aalborg, Denmark; Phone +45 9940 8503; E-mail: phn@bio.aau.dk.

16 Abstract

17 Anaerobic digestion (AD) is a key technology at many wastewater treatment plants
18 (WWTPs) for converting surplus activated sludge to methane-rich biogas. However, the
19 limited number of surveys and the lack of comprehensive data sets have hindered a deeper
20 understanding of the characteristics and associations between key variables and the
21 microbiome composition. Here, we present a six-year survey of 46 anaerobic digesters,
22 located at 22 WWTPs in Denmark, which is the largest known study of the microbial
23 ecology of AD at WWTPs at a regional scale. For three types of AD (mesophilic,
24 mesophilic with thermal hydrolysis pretreatment, and thermophilic), we present the
25 typical value range of 12 key parameters including operational variables and performance
26 parameters. The bacterial and archaeal microbiomes were analyzed at species-level
27 resolution using amplicon sequencing in >1,000 samples and the new ecosystem-specific
28 MiDAS 3 reference database. We detected 42 phyla, 1,600 genera and 3,584 species in
29 the bacterial microbiome, where 70% of the genera and 93% of the species represented
30 uncultivated taxa that were only classified based on MiDAS 3 *denovo* placeholder
31 taxonomy. More than 40% of the 100 most abundant bacterial species did not grow in the
32 digesters and were only present due to immigration with the feed sludge. Temperature,
33 ammonium concentration, and pH were the main drivers shaping the microbiome clusters
34 of the three types of ADs for both bacteria and for archaea. Within mesophilic digesters,
35 feed sludge composition and other key parameters (organic loading rate, biogas yield, and
36 ammonium concentration) correlated with the growing bacterial microbiome.
37 Furthermore, correlation analysis revealed the main drivers for specific species among
38 growing bacteria and archaea, and revealed the potential ecological function of many
39 novel taxa. Our study highlights the influence of immigration on bacterial AD
40 microbiome. Subsetting the growing microbes improves the understanding of the

41 diversity and main drivers of microbiome assembly, and elucidates functionality of
42 specific species-level microorganisms. This six-year survey provides a comprehensive
43 insight into microbiome structure at species level, engineering and ecological
44 performance, and a foundation for future studies of the ecological
45 significance/characteristics and function of the novel taxa.

46 Introduction

47 Anaerobic digestion (AD) is successfully employed worldwide to convert organic
48 feedstock into biogas by anaerobic mixed microbial communities. As a key technology
49 at wastewater treatment plants (WWTP), AD is used to reduce and stabilize the primary
50 and waste-activated sludge by generating methane for bioenergy production. Moreover,
51 AD can be used as a platform for the recovery of value-added compounds (e.g.,
52 phosphorus, nitrogen, volatile fatty acids) [1,2]. Thus, it is an important step in the
53 development of circular economy at the WWTPs. The conversion of organic feedstock is
54 carried out by the AD microbiome, a complex network of hydrolyzing and fermenting
55 bacteria, specialized acidogenic and acetogenic syntrophs, and methanogenic archaea [3],
56 which is shaped by stochastic (birth-death immigration) and deterministic (microbial
57 competition, operation and environment) factors [4,5]. Hence, a good understanding of
58 the microbial ecology in digesters is essential for informed control and manipulation of
59 the process for optimal performance.

60 AD harbours a complex microbial network which is ideal for identifying diversity trends
61 in constrained microbial community structures. Research has shown that the operational
62 parameters, including temperature, substrate type, organic loading rate (OLR), and sludge
63 retention time (SRT) are vital factors for determining the microbiome structure [6–12].
64 Other parameters, such as ammonia concentration and salinity, are also thought to be
65 significant drivers shaping the microbiome [7,13–15]. Additionally, the microorganisms
66 immigrating with the feed sludge should not be overlooked. Most of them do not grow or
67 contribute to the ecological functions in the system, but they still account for a significant
68 fraction of sequencing reads identified by 16S rRNA gene amplicon sequencing [7,9,13].

69 However, most of these findings are based on investigations across various AD substrate
70 types, such as manure, food waste, and wastewater sludge, where large differences in
71 growth conditions are observed. Whether the same drivers are also important among
72 digesters at WWTPs is unclear. The AD performance can be highly variable between
73 different WWTPs, but how this links to different microbiomes and growth conditions is
74 poorly described for full-scale systems.

75 The quantitative relationships between specific microorganisms and key parameters in
76 AD can be evaluated by multiple linear regression (MLR). Most studies have focused on
77 linear associations between methanogenic populations (i.e., characterized by the *mcrA*
78 gene) and specific methanogenic activities [17–20]. However, the traditional MLR fails
79 when the number of predictors is comparable to, or larger than, the number of
80 observations, and when there is high collinearity in predictors. Projection-based methods
81 for analysis of multivariate data, such as Partial Least Squares (PLS) regression, stand as

82 promising techniques to evaluate the links between specific microorganisms and key
83 parameters, lessening the shortcomings of traditional methods [21].

84 To provide insightful links between the AD microbiome and its performance, it is crucial
85 to obtain a high phylogenetic resolution and good taxonomic classification at all ranks. A
86 high phylogenetic resolution can be obtained by using amplicon sequence variants (ASVs)
87 [22,23] instead of operational taxonomic units (OTUs) typically clustered at 97%
88 similarity thresholds, and by using an ecosystem-specific, high-quality 16S rRNA gene
89 reference database for taxonomic classification. We have developed MiDAS 3, a
90 comprehensive ecosystem-specific reference database for activated sludge and anaerobic
91 digesters which provides a taxonomic classification at all ranks for all sequences based
92 on an improved and automated classification system (AutoTax) [24,25]. The MiDAS 3
93 reference database is based on full-length 16S rRNA gene ASVs (FL-ASVs) obtained
94 from Danish WWTPs and digesters, but can be applied to similar systems worldwide [24].
95 MiDAS 3 improves the classification of prokaryotic microorganisms found in AD
96 compared to other public reference databases (SILVA [26], Greengenes [27], and RDP
97 [28]), which lack reference sequences for many taxa and high taxonomic resolution, often
98 resulting in poor classification (**Figure S1**). Application of MiDAS 3 for the study of AD
99 communities offers a possibility of finding the link between identity and function of
100 species-level taxa. Species names provide stable taxa identifiers independent of the data
101 set, thus, allowing cross-study comparisons.

102 The aims of our study are threefold. Firstly, we describe the typical operational
103 parameters and performance values of three different types of AD at WWTPs (i.e.,
104 mesophilic AD, mesophilic AD with pre-treatment (thermal hydrolysis) of waste
105 activated sludge, and thermophilic AD). Secondly, we present the microbial communities
106 in the AD systems (with focus on the growing microbes), for the first time at species level,
107 and make this publicly available on the MiDAS website
108 (<https://www.midasfieldguide.org/guide>). And thirdly, by focusing on species-level
109 microbiome, we analyse the correlations between key AD parameters and microbiome
110 structure in mesophilic digesters, which are the most common digesters in Denmark at
111 WWTPs.

112 **Methods**

113 **Anaerobic digesters and sample collection**

114 The survey was conducted during the period 2011 – 2016 in 46 anaerobic digesters at 22
115 WWTPs across Denmark, which were operated under mesophilic (MAD), mesophilic
116 with thermal hydrolysis pretreatment of feedstock (THP-MAD), or thermophilic (TAD)
117 conditions (see **Table S1** for information of digesters). During the six years of survey, all
118 plants reported minor fluctuations in substrate amounts and composition, but no major
119 changes of operating conditions were introduced, except for Aaby and Aalborg East,
120 which switched from mesophilic to thermophilic operation (**Table S1**). A total of more
121 than 50,000 observations, including operational, physicochemical, and performance
122 parameters, except volatile fatty acids (VFAs), were obtained from the records of

123 individual plants. Each key variable had at least 1,087 observations, except VFAs (**Table**
124 **1**).

125 The digester sludge samples were obtained 2-4 times a year during the investigation
126 period, and the VFA samples were collected 2-5 times from each studied digester during
127 2016. All samples were transported to the laboratory within 24 h and processed
128 immediately upon arrival. After homogenization, the biomass samples were stored as 2
129 mL aliquots at -80°C before DNA extraction. Samples for VFA analysis were filtered
130 with 0.22 µm filters (Frisenette, Knebel, Denmark) and stored at -20°C until analysis,
131 which is described elsewhere [29].

132 **DNA extraction, 16S rRNA gene amplicon sequencing, and bioinformatics 133 processing**

134 The microbial communities of a total of 1,010 AD sludge samples (418 for archaea and
135 592 for bacteria) were analyzed using 16S rRNA gene amplicon sequencing. 50 µl AD
136 sample were used for DNA extraction with the FastDNA® Spin Kit for soil (MP
137 Biomedicals, Solon, OH, USA), following the optimized protocol for anaerobic digesters
138 by Kirkegaard et al. [30]. The library preparation for 16S rRNA amplicon sequencing was
139 performed as described in Kirkegaard et al. [10], targeting the V1-3 variable regions for
140 bacteria and V3-5 variable regions for archaea. The bacterial primers used were 27F
141 (AGAGTTTGATCCTGGCTCAG) [31] and 534R (ATTACCGCGGCTGCTGG)[32],
142 which amplify a DNA fragment of ~500 bp of the 16S rRNA gene (V1–3). The archaeal
143 primers used were 340F (CCCTAHGGGGYGCASCA) [33] and 915R
144 (GWGCYCCCCCGYCAATT) [33], which amplify a DNA fragment of ~ 560 bp of the
145 16S rRNA gene (V3–5). The amplicon libraries were paired-end sequenced (2×300 bp)
146 on the Illumina MiSeq as described by Albertsen et al. [34].

147 The archaeal and bacterial read data were analyzed separately using USEARCH
148 (v.11.0.667) [35]. For the V1-3 amplicons raw fastq files were filtered for phiX sequences
149 using -filter_phix, trimmed to 250 bp using -fastx_truncate -truncen 250, and quality
150 filtered using -fastq_filter with -fastq_maxee 1.0. The sequences were dereplicated using
151 -fastx_uniques with -sizeout -relabel Uniq. ASVs were generated using UNOISE3 [36],
152 and ASV-tables were created by mapping the raw reads to the ASVs using -otutab with
153 the -zotus and -strand both options. Taxonomy was assigned using the MiDAS 3 reference
154 database [24,25] using syntax with the -strand both and -syntax_cutoff 0.8 [37]. The V3-5
155 amplicon data were analyzed in the same way except that only the reverse read was used
156 and the primer binding site was removed during the trimming using -fastx_truncate -
157 stripleft 18 -truncen 250.

158 **Data processing and statistical analysis**

159 Downstream statistical analyses and visualization were mostly performed in the R
160 environment (v3.6.2) [38] using *ampvis2* (v2.5.8) [34] and *ggplot2* (v3.2.1) [39], unless
161 indicated otherwise. Non-parametric *dunn.test* was used to identify significant differences
162 between AD types. The correlations between all the variables were explored by Spearman
163 correlation, where correlations greater than ± 0.5 and false discovery rate (FDR) corrected
164 $P > 0.05$ were visualized in Gephi (v0.9.2) [40], using Force Altas2 and manual tweaking

165 to generate the network. For sequence data, samples were randomly subsampled to 10,000
166 sequences per sample, yielding a final dataset of 402 archaeal and 564 bacterial samples.
167 For the growing bacteria datasets, after removing the non-growing ASVs from ASVtable,
168 samples were also randomly subsampled to 10,000 sequences per sample for downstream
169 analysis and comparison. Boxplot and heatmaps were made by the *amp_boxplot* and
170 *amp_heatmap* function in *ampvis2*. Alpha diversity was calculated by *amp_alpha*
171 function in *ampvis2*. The linear regression between alpha diversity (using Shannon's
172 index) and each operational and performance variable was used to pick the key variables
173 most correlated. Weighted uniFrac distance, calculated by *beta_diversity.py* script in
174 QIIME (v1.9.0) [41], was applied for all beta diversity comparisons. For ordination
175 visualizations, the non-metric multidimensional scaling (NMDS) was performed by
176 *amp_ordinate* in *ampvis2* to show the dissimilarities of microbial profiles. Based on
177 weighted uniFrac distance matrix, ANOSIM was applied to assess similarities for
178 categorical variables using *compare_categories.py* in QIIME with 999 permutations. A
179 PERMANOVA analysis using adonis in QIIME was used to describe the strength and
180 significance for continuous variables. The significant difference of species between two
181 groups of feed sludge was explored by Wilcoxon rank-sum test.

182 PLS regression was performed using R package *mdatools* v0.10.1 [21] to validate
183 quantitative relationship between operational and performance parameters, and the
184 microbial community, as well as to identify specific microbes which correlate to each
185 variable the most. All bacterial species with median relative abundance $\geq 0.01\%$ and
186 archaeal ASVs with median relative abundance $\geq 0.05\%$ were used to perform the PLS
187 analysis. The model was trained using all samples and validated by segmented cross-
188 validation (CV) with systematic splits (venetian blinds). Determination coefficient (R^2)
189 and root mean square error (RMSE) were used to assess performance of the model. The
190 contribution of individual predictors was evaluated using regression coefficients and
191 corresponding inferential analysis carried out by Jack-Knifing approach [42].

192 Results and discussion

193 Characterization of key parameters of AD

194 Key operational and performance parameters of the 46 anaerobic digesters during the six-
195 year survey are summarized in **Table 1**. The digesters are classified into three types, based
196 on the operational temperature and pretreatment of the feed sludge. MAD is the most
197 common configuration (78% of all digesters) followed by TAD (15%) and THP-MAD
198 (7%). The most common digester type is single-stage continuously stirred tank reactor
199 (CSTR). The anaerobic digesters surveyed were running stably without major process
200 complications for six years, therefore common ranges of operation and performance
201 conditions are described for each digester type. As presented in **Table 1** and described
202 below, values of several environmental parameters are very different from other AD
203 systems treating manure, crops, food waste, and industrial waste [7,11,15,43–47], with
204 generally lower or much lower values of total ammonia nitrogen (TAN) and level of
205 VFAs.

206 The median temperature values of the three types of digesters were 38.0°C, 38.6°C, and
207 53.6°C, for MAD, THP-MAD, and TAD, respectively. Other operational variables (OLR
208 and SRT) and the performance parameters (pH, TAN, alkalinity, TS, VS, biogas yield,
209 and methane content) were found to be significantly different across all three types of AD
210 (**Figure S2**). For more details on the description of each parameter, please see **Additional**
211 **file 2**. In general, the same overall correlations between operational and performance
212 parameters across digesters treating different types of substrates could also be observed
213 specifically for digesters among WWTPs. Strong positive correlations (Spearman, $r > 0.7$,
214 false discovery rate (FDR) $P < 0.05$) were observed between TAN and TS or VS, OLR
215 and alkalinity, and methane production and SRT (**Figure S3**). Strong negative
216 correlations between the OLR and methane production and biogas yield were also
217 revealed (Spearman, $r > 0.65$, FDR $P < 0.05$), and between methane production and TAN
218 (**Figure S3**), indicating that these operational variables are linked to the performance of
219 the digesters. It is interesting that VFAs only related weakly to SRT and the ratio of VS
220 to TS, which have previously been considered as important variables [48]. This may be
221 due to a general low concentration range in the digesters and low loading.

222 **Table 1. Operational variables and performance parameters: Intervals and median**
223 **values for ADs at WWTPs in Denmark.**

Category	Variable	Unit	MAD*		THP-MAD*		TAD*	
			Interval ¹	Median	Interval	Median	Interval	Median
Operational variables	Temperature	°C	35.6 ~ 39.9	38.0	38.2 ~ 39.0	38.6	51.1 ~ 55.40	53.6
	OLR ²	kg VS/m ³ ·d	0.84 ~ 1.13	0.96	1.66 ~ 2.30	2.04	1.63 ~ 2.49	2.15
	SRT*	Day	24.8 ~ 35.6	29.4	27.3 ~ 34.9	30.1	15.8 ~ 20.7	17.3
Performance parameters	TS*	g/L	21.1 ~ 38.4	31.0	41.1 ~ 65.9	44.8	31.2 ~ 39.0	35.8
	VS*	g/L	12.1 ~ 19.9	16.2	25.9 ~ 34.0	27.7	21.0 ~ 25.5	23.6
	VS	TS%	56.0 ~ 61.6	58.6	54.0 ~ 63.5	60.2	57.0 ~ 60.9	58.0
	pH	-	7.06 ~ 7.38	7.19	7.64 ~ 7.86	7.75	7.50 ~ 7.80	7.70
	TAN	mg N/L	603 ~ 972	745	2691 ~ 3100	2888	1070 ~ 1430	1215
	Alkalinity	mM	50.0 ~ 73.0	60.8	148 ~ 186	168.6	67.9 ~ 87.7	78.4
	Total VFA*	mM	0.28 ~ 1.11	0.50	0.45 ~ 2.34	0.73	0.92 ~ 2.18	1.30
	Acetate	mM	0.10 ~ 0.40	0.21	0.25 ~ 0.44	0.30	0.53 ~ 1.18	0.79
	Biogas yield ²	Nm ³ /kg VS	0.39 ~ 0.53	0.46	0.38 ~ 0.56	0.49	0.25 ~ 0.36	0.29
	Methane content	%	61.0 ~ 63.5	61.7	63.0 ~ 65.0	65.0	53.7 ~ 64.3	57.6
	Methane production ³	Nm ³ / m ³ ·d	-	0.27	-	0.65	-	0.36

224 ¹ Interval shows the range of first quartile and third quartile of each variable.

225 ² OLR and biogas yield are normalized using an average volatile solids value of influent feed (74.5%).

226 ³ Methane production is calculated on median value of biogas yield, OLR, and methane content.

227 * MAD = mesophilic, THP-MAD = mesophilic with thermal hydrolysis pretreatment, TAD = thermophilic, OLR = organic loading
228 rate, SRT = solids retention time, TS = total solids, VS = volatile solids, TAN = total ammonia nitrogen, Total VFA = total volatile
229 fatty acid.

230

231 Like many other full-scale plants, running at low OLR and long SRT of the digesters
232 surveyed, which is referred as “suboptimal” operational conditions, may lead up to a 30%
233 profitability loss [46,49]. Increasing the OLR seems promising, but there may be a
234 number of operational problems which need to be considered, such as foaming and
235 acidosis, due to the imbalance between operational and microbial processes. Thus, a better
236 understanding of microbial communities and their function may help to control or
237 manipulate the processes that decrease the potential risks of operational failures.

238 **Bacterial and archaeal microbiomes**

239 We obtained 33,047 bacterial and 878 archaeal unique ASVs, which were classified and
240 assigned using sintax and the MiDAS 3 database. Thus, a total of 42 phyla, 1,600 genera,
241 and 3,584 species were detected in the bacterial microbiome, where 1,117 (70%) genera
242 and 3,336 (93%) species were novel and could only be assigned genus and species name
243 based on the MiDAS 3 *denovo* placeholder taxonomy. For archaea it was not possible to
244 analyze the methanogenic archaea at the species level because the phylogeny of most of
245 these species cannot be resolved using the 16S rRNA gene, even with full-length
246 sequences [24]. As a result, only 26 species were classified and most of the archaeal
247 population are shown at ASV level.

248 AD at WWTPs are complex systems, as they receive a substantial amount of
249 microorganisms via feed streams (primary sludge, PS, or surplus activated sludge, AS).
250 Many of these microorganisms are not growing in the digester, presumably inactive or
251 dying off [10,13,50]. The growing and non-growing microorganisms were identified
252 according to the ratio of read abundances in digester and feed as described by Kirkegaard
253 et al. [10]. The bimodal distribution of ratios was split at a ratio of around 10 (**Figure S4**),
254 showing two clearly separated groups of ASVs. The group with a ratio >10 represents
255 ASVs enriched in digesters compared to the feed sludge, here designated as “growing
256 microorganisms”. The group with a ratio <10 represents ASVs with unchanged or lower
257 relative read abundance in digesters, compared to the feed sludge, here designated as
258 “non-growing microorganisms”. Thus, combined with median relative abundance across
259 samples in each type of AD, the total ASVs (>0.01% median relative abundance) were
260 divided into four groups, growing/non-growing ASVs with high abundance (>0.1%) and
261 growing/non-growing ASVs with low abundance (<0.1%). It was observed that the
262 growing highly abundant ASVs only accounted for 7.6%, 23.2%, and 9.4% of the total
263 ASV counts in MAD, THP-MAD, and TAD, respectively (**Fig. 1**). However, the
264 proportion of relative abundances of these growing highly abundant ASVs were large, at
265 38.8%, 85.3%, and 50.9% in MAD, THP-MAD, and TAD, respectively. This suggests
266 that the performance and functionality of AD might be driven by only a small number of
267 the microbial phylotypes detected by amplicon sequencing.

268 The five most abundant bacterial phyla were Firmicutes, Proteobacteria, Chloroflexi,
269 Actinobacteria, and Bacteroidetes, accounting for 75.7% (median value) of all amplicon
270 sequences across all samples, and these phyla are typical for digesters at WWTPs
271 [7,15,43,51–54]. However, the three types of AD showed variations in the dominant
272 bacterial taxa, especially at genus level (**Figure S5**). Among the 25 most abundant species,
273 11 species in MAD and 9 species in TAD belonged to the group of non-growing
274 microorganisms (**Fig. 2A and 2B**). These included species in genera belonging to the
275 polyphosphate-accumulating organisms (PAO) *Tetrasphaera*, the putative PAO
276 *Dechloromonas* [55], the filamentous genus *Ca. Microthrix* [56], and the genera
277 *Romboutsia*, and *Trichococcus*. These all belong to the top-most abundant reported
278 genera in activated sludge in Danish WWTPs [25], thereby indicating carry-over to the
279 digesters with the feed sludge. Since the top100 species in MAD and TAD, respectively,
280 are very similar across the digesters, these lists can be used as a representative reference

281 of abundant growing and non-growing organisms in digesters at WWTPs across the world
282 (**Figure S6 and S7**). These results demonstrate that surprisingly many, 44% and 54% of
283 the species were non-growing in MAD and TAD, respectively. The top 25 species in
284 THP-MAD all belonged to growing microorganisms in good agreement with the presence
285 of THP pretreatment, which causes a decay of essentially all organisms coming with the
286 feed sludge (**Figure S8A**).

287 The growing microorganisms are considered to be responsible for the most important
288 ecological functions within AD. Among the dominant growing bacterial species there
289 were many known fermenters, such as species belonging to the genera *Thermovirga*, *Ca.*
290 *Fermentibacter*, and *Leptolinea* in MAD, and *Coprothermobacter* and *Acetomicrobium*
291 in TAD. There were also syntrophic bacteria, such as members of *Ca. Cloacimonas* [57]
292 and *Syntrophorhabdus* in MAD. However, a large fraction of the most abundant growing
293 species were novel taxa without any known function. They were identified by MiDAS 3
294 species-level taxonomy and given robust placeholder names until characterized in more
295 detail, enabling across-study comparisons of AD microbiome at high taxonomic
296 resolution [24]. Due to the high relative abundance, some genera are of special interest:
297 *midas_g_12* (family Prolixibacteraceae), *midas_g_19* (family Bacteroidetes vadinHA17),
298 *midas_g_156* (family Anaerolineaceae), and *midas_g_789* (family Anaerolineaceae) in
299 MAD; *midas_g_88* (family Syntrophomonadaceae), *midas_g_112* (order MBA03), and
300 *midas_g_16* (family Lentimicrobiaceae) in TAD, and *midas_g_13* (order D8A-2) in THP-
301 MAD. Some of these genera encompass very abundant species, especially in the family
302 Anaerolineaceae (up to 8% median abundance): *midas_s_156*, *midas_s_876*,
303 *midas_s_956*, *midas_s_1462*, *midas_s_467*, *midas_s_1625*. These abundant and novel
304 taxa should be investigated in future studies, as their physiology and ecological role in
305 AD are completely unknown while likely important.

306 Moreover, compared with MiDAS 2 taxonomy (which was the curated version of Silva
307 taxonomy) [58], MiDAS 3 provides a much higher resolution to classify sequences and
308 introduces species-level names for the first time for the abundant microorganisms in AD
309 ecosystem. For example, genus T78 (family Anaerolineaceae) in MiDAS 2 encompassed
310 sequences that are split into *midas_g_156* and *midas_g_467* in MiDAS 3, both being the
311 abundant genera mentioned above. These genera are both diverse, each having three
312 abundant species present in MAD (**Figure S9**). Also, *Ca. Cloacimonas* and
313 *Pelotomaculum* and the newly discovered syntrophic genus *midas_g_995* [29] had high
314 species diversity as well, with several abundant species with random distribution (**Figure**
315 **S9**).

316 Euryarchaeota was the dominant archaea in the digesters (99.9%, median value). The
317 acetoclastic genus *Methanothrix* (previously named *Methanosaeta*) dominated in MAD
318 (71.8%) and THP-MAD (93.8%), whereas the genera *Methanothermobacter* (70.7%) and
319 *Methanosarcina* (24.8%) dominated in TAD (**Figure S10B**). *Methanosarcina* was in very
320 low abundance in MAD (0.1%) and THP-MAD (0.01%), in contrast to other mesophilic
321 full-scale studies of manure-based AD where it was dominant [7,53,59]. However, the
322 low concentrations of VFAs (<1 mM) in the mesophilic AD may explain why
323 *Methanothrix* dominated [60]. The hydrogenotrophic methanogenic *Methanoculleus* was

324 the predominant genus (4.2%) in THP-MAD, which is in line with other lab-scale and
325 pilot-scale THP digesters studies [61,62].

326 Acetoclastic and hydrogenotrophic methanogenic species/ASVs were quite abundant in
327 all the types of AD (**Fig. 2C, 2D, and Figure S8B**). *g_Methanothrix_ASV1* was
328 dominant in both MAD and THP-MAD, followed by *midas_s_1190* (genus *Methanolinea*)
329 and *g_Methanolinea_ASV6* in MAD and *midas_s_880* (genus *Methanoculleus*) in THP-
330 MAD. *Methanothermobacter tenebrarum* and *Methanosaeca thermophila* species were
331 the second most abundant species in TAD (**Fig. 2**).

332 **Microbial diversity in different AD types**

333 The use of common measures for richness and diversity in the digesters surveyed has only
334 limited value, as abundant immigrating bacteria, likely inactive or dying off without any
335 functional role in the systems, will influence the diversity measures and produce
336 misleading results. This is illustrated by comparing the diversity measures calculated for
337 all bacteria and for the growing bacteria only (**Fig. 3A**). When the non-growing fraction
338 was removed, the median values of observed ASVs decreased from 1935 to 928, 1486 to
339 534, and the median values of Shannon index from 6.22 to 5.11 and 5.59 to 4.33 in MAD
340 and TAD, respectively (**Fig. 3A**). THP-MAD only had a minor change in observed ASVs
341 (from 832 to 741) and the median Shannon index (4.47 and 4.63, respectively), reflecting,
342 as expected, that these communities were not strongly influenced by immigration. The
343 adjusted diversity measures showed the same order of magnitude decrease for archaea
344 (**Figure S11**) with THP-MAD between MAD and TAD. The measures also showed that
345 higher temperature harbored fewer number of microbes in accordance to other full-scale
346 surveys [15,51], but that the exact values are strongly dependent on the inclusion of the
347 immigrating microbes. Higher alpha diversity measures for bacterial communities
348 compared with archaea is in agreement with other full-scale WWTPs studies [15,43,51].
349 The diversity in thermophilic AD has been shown to be lower than in mesophilic digesters
350 [63–65], which is also supported by our data.

351 The total bacterial (including growing and non-growing fraction) and archaeal
352 microbiome seemed relatively stable in each digester across all 22 WWTPs during the
353 six-year survey as indicated by tight clustering as visualized by non-metric
354 multidimensional scaling (NMDS) (**Figure S12**). This is also reported from other time-
355 series studies of full-scale digesters mainly treating manure, agricultural waste, and
356 municipal solid waste [7,43], suggesting that overall stable microbiomes are common in
357 full-scale digesters during steady-state operation. However, as a major part of the
358 microorganisms are immigrants, they may strongly affect the betadiversity measures.
359 Therefore, it is important to compare the diversity of both the total and the growing
360 fraction of the population. The dissimilarity among plants seemed the same considering
361 the community structure of the total and growing bacteria in MAD (ANOSIM; Total
362 bacteria: $R = 0.65, P = 0.001$; Growing bacteria: $R = 0.63, P = 0.001$) and THP-MAD
363 (ANOSIM; Total bacteria: $R = 0.45, P = 0.001$; Growing bacteria: $R = 0.49, P = 0.001$).
364 However, the growing bacterial community in TAD became more similar across plants
365 compared to the total bacterial population (ANOSIM; Total bacteria: $R = 0.64, P = 0.001$;
366 Growing bacteria: $R = 0.40, P = 0.001$). This shows that the inclusion of non-growing

367 bacteria in microbiome analyses of TAD may lead to misleading results and erroneous
368 conclusions.

369 Analysis of beta diversity of the communities present in different AD types revealed three
370 distinct clusters corresponding to MAD, THP-MAD, and TAD (**Fig. 3B and Figure**
371 **S13A**). Clear separation dictated by AD type was evident for all bacteria (ANOSIM: $R = 0.95$, $P = 0.001$), the growing bacteria (ANOSIM: $R = 0.97$, $P = 0.001$), as well as the
372 archaeal microbiome (ANOSIM: $R = 0.83$, $P = 0.001$), reflecting the huge effects of
373 operational conditions on the resulting variation in the microbiomes. Permutational
374 multivariate analyses of variance showed that TAN contributed to shaping the structure
375 of the total bacterial microbiome (adonis: $R^2 = 32\%$, $P = 0.001$) (**Figure S13B**), which
376 has also been observed in full-scale digesters treating different kinds of substrates [7]. In
377 contrast to the bacterial microbiome, the overall structure of the archaeal microbiome was
378 separated mainly by temperature (adonis: $R^2 = 66\%$, $P = 0.002$), with a separate cluster
379 for THP-MAD alongside MAD (**Figure S13C**). pH was the second factor influencing the
380 archaeal microbiome (adonis: $R^2 = 27\%$, $P = 0.002$), which may explain the separated
381 cluster of THP-MAD from MAD (**Figure S13D**).

383 **Main drivers of MAD microbiome**

384 Since most digesters surveyed were MAD, we further applied the correlation analysis
385 between key parameters and microbial diversity and structure to determine the main
386 drivers, with special focus on the growing bacterial microbiome, as non-growing
387 microorganisms may mask the influence of key drivers on the active microbiome in
388 correlation analyses. In general, bigger difference was observed on linear regression of
389 key parameters against alpha diversity between the total and growing bacterial
390 microbiomes, compared with permutational multivariate analysis of betadiversity (**Table**
391 **S2** and **Table S3**).

392 It is well-known that temperature is a very important factor for shaping the microbial
393 diversity and community structure in full-scale digesters [7,15,43], but it is less clear to
394 what extent it is for mesophilic AD at WWTPs. In our study, the temperature range in
395 MAD was small (35.6-39.9) and was only considered to be most important to the total
396 bacterial alpha diversity in MAD (25%, linear regression, FDR $P < 0.001$, **Table S2**), but
397 not the alpha diversity of growing bacteria (16%, FDR $P < 0.001$). This indicates that
398 temperature may not be the most important factor in MAD. Instead, the correlation
399 coefficient of OLR improved significantly by subsetting the growing bacterial alpha
400 diversity (31%, $P < 0.001$) compared to the total bacterial alpha diversity (9%, $P > 0.05$).
401 OLR also shaped the microbiome structure (beta diversity) of growing bacteria (adonis:
402 $R^2 = 21\%$, $P = 0.001$, **Table S3**). Although OLR is widely accepted as a deterministic
403 factor for any type of AD microbiome [66-69], our study strengthened it when OLR was
404 only correlated with growing bacteria. Moreover, the biogas yield exhibited strong
405 correlation with the growing bacterial microbiome both on alpha diversity (46%, $P <$
406 0.001) and beta diversity (adonis: $R^2 = 31\%$, $P = 0.001$), as well as archaeal beta diversity
407 (adonis: $R^2 = 23\%$, $P = 0.008$), supporting the observation that AD performance depends
408 on the activity of the microbiome [70]. Similarly, TAN was observed to be more
409 correlated to growing bacterial alpha diversity compared with the total bacterial

410 population (**Table S2**). Regarding the archaeal microbiome, no strong correlation was
411 found between parameters and alpha diversity in MAD. However, apart from biogas yield,
412 acetate concentration (adonis: $R^2 = 18\%$, $P = 0.04$) was also found to have significant
413 correlation with the archaeal microbiome structure.

414 Samples from MAD digesters treating only surplus AS and without PS (Fornæs,
415 Mariagerfjord, and Soeholt) formed a small separate cluster, compared to MAD treating
416 a mixture of both types of substrates for all bacteria (ANOSIM: $R = 0.44$, $P = 0.001$,
417 **Figure S14A**) and for the growing bacteria (ANOSIM: $R = 0.57$, $P = 0.001$, **Fig. 3C**).
418 The higher dissimilarity of growing bacteria in MAD supports the observation that
419 substrate characteristics (e.g., biodegradability, composition, concentration) from PS
420 shape the growing bacterial community structure [7,15]. This is different from the
421 growing bacteria in the three types of AD, which is mainly driven by operational
422 parameters (**Fig. 3B**). While for all bacterial communities, the relative abundance of 18
423 of the 25 most abundant species showed a significant difference between the two clusters
424 depending on the feed sludge (Wilcoxon rank-sum test, $P < 0.05$, **Figure S14B**). Non-
425 growing species in digesters but abundant in AS (i.e., species belonging to genus
426 *Tetrasphaera*, *Ca. Microthrix*, or *Dechloromonas*) were found in higher relative
427 abundance in MAD treating only AS compared to MAD treating AS and PS. These results
428 underline that besides substrate characteristics, the immigrating bacterial load has a strong
429 impact on the total bacterial microbiome in AD. Additionally, we also observed the
430 influence of feed sludge on archaeal community (**Figure S15A**), with significant
431 difference between the digesters with different feed sludge (ANOSIM: $R = 0.23$, $P =$
432 0.001). It is interesting to see that the species belonging to genus *Methanolinea* were rare
433 in the digesters only fed with AS (**Figure S15B**).

434 **Relationship between MAD microbiome and its driving factors predicted by PLS
435 regression model**

436 We applied PLS regression to predict key operational variables and performance
437 parameters and their relationship to the microbiome in MAD. Separate PLS models were
438 built on the bacterial microbiome at species level and archaeal ASVs with each factor (for
439 bacteria: temperature, OLR, TAN, and biogas yield; for archaea: temperature, TAN,
440 acetate, and biogas yield). Very good prediction accuracy was observed on the bacterial
441 microbiome, where the CV R^2 of all four PLS models exceeded 0.85 (**Fig. 4**). However,
442 none of the models based on archaeal ASVs had the R^2 over 0.80, except for biogas yield
443 (**Fig. 4**). PLS regression models were also carried out on pH and SRT, since they are
444 important AD parameters (**Figure S16 and S17**). The growing bacterial species and
445 archaeal ASVs, which most significantly contributed to each PLS regression model (the
446 contribution was estimated using inferential statistics for corresponding regression
447 coefficients, $P < 0.05$), for both positive and negative contributions, are shown in **Fig. 5**.

448 Most growing bacterial species exhibiting significant correlations were represented by
449 novel taxa (**Fig. 5A**). Species belonging to the same genus were correlated to different
450 operational or performance parameters, such as was the case with two species in family
451 Anaerolineaceae (*midas_s_467* and *midas_s_1462* belonging to genus *midas_g_467*).
452 The positive correlation of *midas_s_467* with TAN and biogas yield, and the negative

453 correlation of midas_s_1462 with temperature and OLR, could explain the abundance
454 variability and trend across MAD (**Figure S9**). Similar observations were found for three
455 species belonging to genus midas_g_12 (family Prolixibacteraceae, phylum
456 Bacteroidetes). The ecological function of these novel species is unknown so the PLS
457 correlation results may provide hypotheses which could aid the design of experiments to
458 reveal the role of novel taxa in AD [71]. Among the known species, *Ca. Brevefilum*
459 *fermentans* showed a positive correlation with TAN, which can indicate a preference or
460 tolerance to slightly higher TAN conditions. This hypothesis is supported by their genome
461 blueprint indicating that *Ca. B. fermentans* can ferment proteinaceous substrates to VFAs
462 with ammonium as a by-product of protein degradation [72]. Additionally, species
463 belonging to the known syntrophic genera *Ca. Cloacimonas*, *Smithella*, *Syntrophomonas*,
464 and *Syntrophorhabdus* were found mostly negatively correlated with TAN and
465 temperature, thereby confirming the high sensitivity of this group to environmental
466 conditions [73–76].

467 Non-growing bacterial species (primarily immigrating with the feed sludge) showed
468 negative correlations to some key parameters (**Figure S18**), especially for biogas yield
469 and SRT, suggesting that they are not directly involved in the conversion of feed stocks
470 to biogas and are probably degraded or washed out of the digesters. This is exemplified
471 by *Tetrasphaera* midas_s_5, the most abundant non-growing species in MAD, and it was
472 negatively correlated with SRT together with *Tetrasphaera elongata* and midas_s_299.
473 *Tetrasphaera* is very abundant in Danish wastewater treatment plants [55] and is
474 introduced into the digester with the waste activated sludge. The negative correlation with
475 the SRT indicates that *Tetrasphaera* is dying off in the digesters despite the potential for
476 surviving or growing under anaerobic conditions as fermenters, and polyphosphate
477 accumulators [77].

478 Correlation results for archaeal ASVs are shown in **Fig. 5B**. Generally, ASVs belonging
479 to the same genus show the same trends. For example, ASVs classified to family
480 Methanosarcinaceae and order Methanosarcinales known as acetoclastic and
481 hydrogenotrophic methanogens, positively correlated with acetate. This is consistent with
482 other findings [78] where *Methanosarcina* was most abundant in digesters with higher
483 acetate concentration. In contrast, most *Methanothrix* ASVs correlated negatively with
484 acetate, supporting the dominance of *Methanothrix* at low acetate concentrations [79].
485 Many *Methanothrix* ASVs also showed negative correlation with TAN, which is in
486 agreement with studies that show that *Methanothrix* is the methanogen most sensitive to
487 ammonia inhibition [80]. It is interesting that even small TAN variations as seen here for
488 Danish digesters (603–972 mg N/L, MAD – **Table 1**) can affect individual *Methanothrix*
489 ASVs in different ways.

490 For hydrogenotrophic methanogens, different ASVs from the same genus or species
491 showed diverse correlations with AD parameters. The second most abundant archaeal
492 species in MAD belonging to genus *Methanolinea* (midas_s_1190) included three ASVs,
493 which correlated with TAN differently suggesting that species microdiversity can
494 influence process performance. The negative correlation of many hydrogenotrophic
495 methanogens with biogas yield, such as *Methanoculleus*, could be due to their ability to

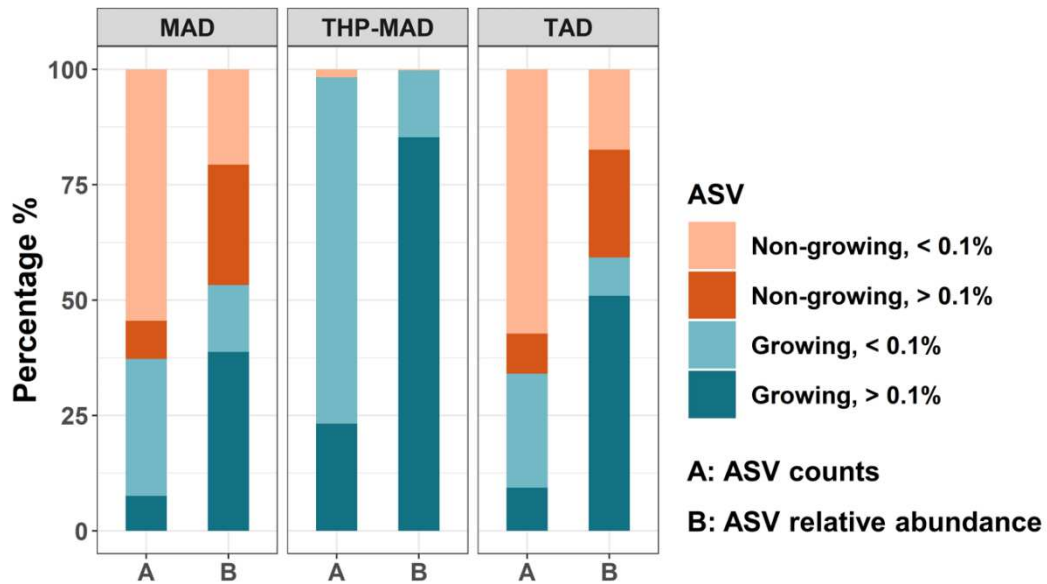
496 survive/compete at sub-optimal AD conditions (e.g., increased TAN) [80] which could
497 translate into lower biogas yields.

498 Overall, the PLS regression models presented enable elucidation of the relationships
499 between important AD parameters and the main drivers shaping AD microbiome at very
500 high resolution. The results for known taxa agree with present knowledge, thus verifying
501 the robustness of the PLS application in microbiome study. Importantly, a combination
502 of the PLS regression with species-level microbial data provides the first insight into
503 potential functional importance of several novel microorganisms, where little or no
504 description of their ecology and physiology is available. Based on our observations,
505 hydrolytic-fermentative bacteria, and acetogenic syntrophs along with archaeal
506 methanogens, all have significant and quantitative relationships with important
507 parameters at MAD. This shows great promise for the improved models, and optimized
508 functional performance of AD.

509 Conclusion

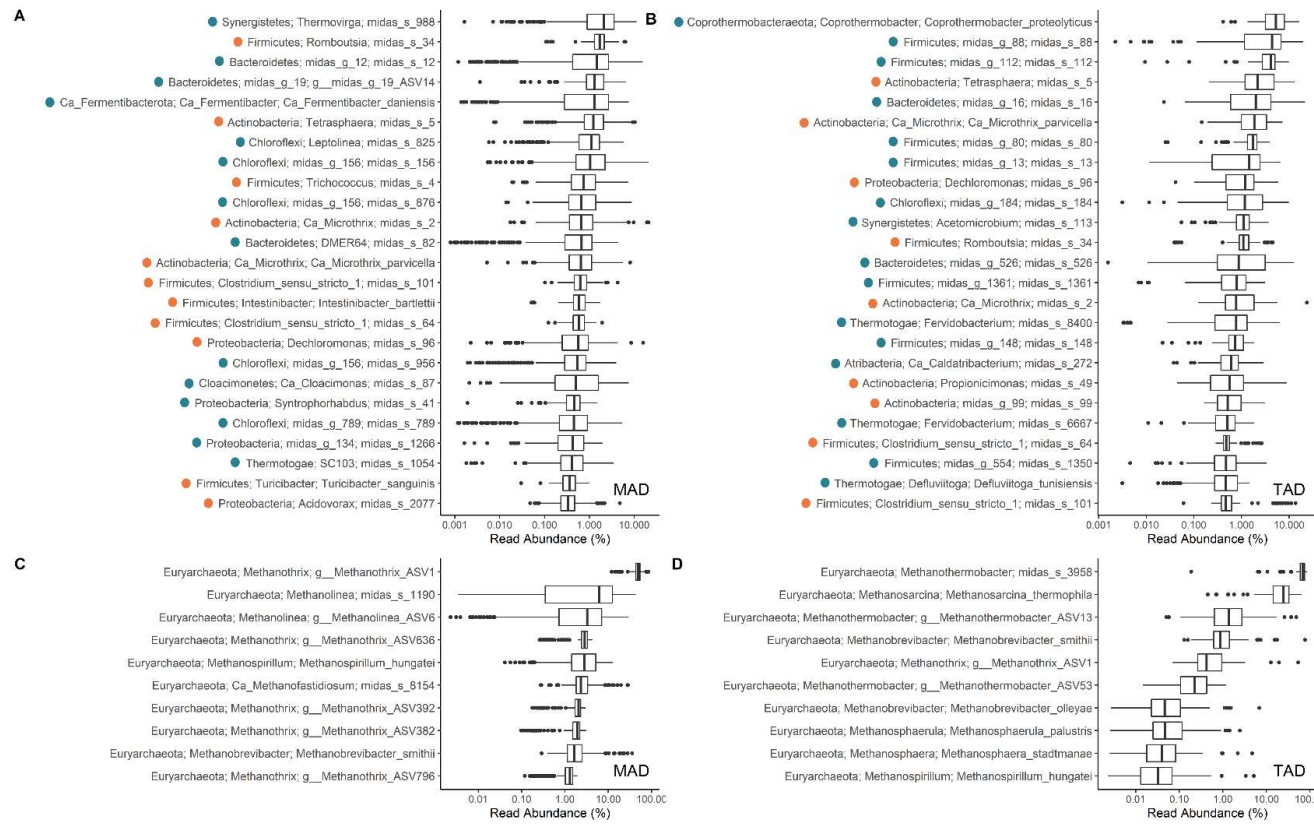
510 A six-year survey of 46 anaerobic digesters located at 22 Danish WWTPs provided a
511 comprehensive overview of typical operational and performance parameters, detailed
512 identification of the AD microbiome at species level, and elucidated relationships
513 between specific taxa and key parameters in AD. The anaerobic digesters surveyed were
514 running stably but operated at low intensity, a common feature across digesters in WWTP.
515 Non-growing species migrating from the feed sludge were abundant in mesophilic and
516 thermophilic AD, but did not seem to contribute to the functionality of AD. In contrast,
517 many growing species were novel and identified using MiDAS 3 taxonomy, and their
518 physiological and ecological roles in AD remains to be described. The microbiome of the
519 three types of AD surveyed (mesophilic, thermophilic, and thermal hydrolysis pre-
520 treatment-mesophilic) showed high stability within plants, forming separate clusters for
521 all bacteria, growing bacteria, and archaea depending on the operational parameters. The
522 variations of growing bacteria within mesophilic digesters were related to organic loading
523 rate, ammonium concentration, feed sludge characteristics, and biogas yield. Multiple
524 correlations between growing bacteria and archaea at species level and key parameters
525 were found, forming a basis for future studies of the ecology and function of novel taxa.

526 **Figures**



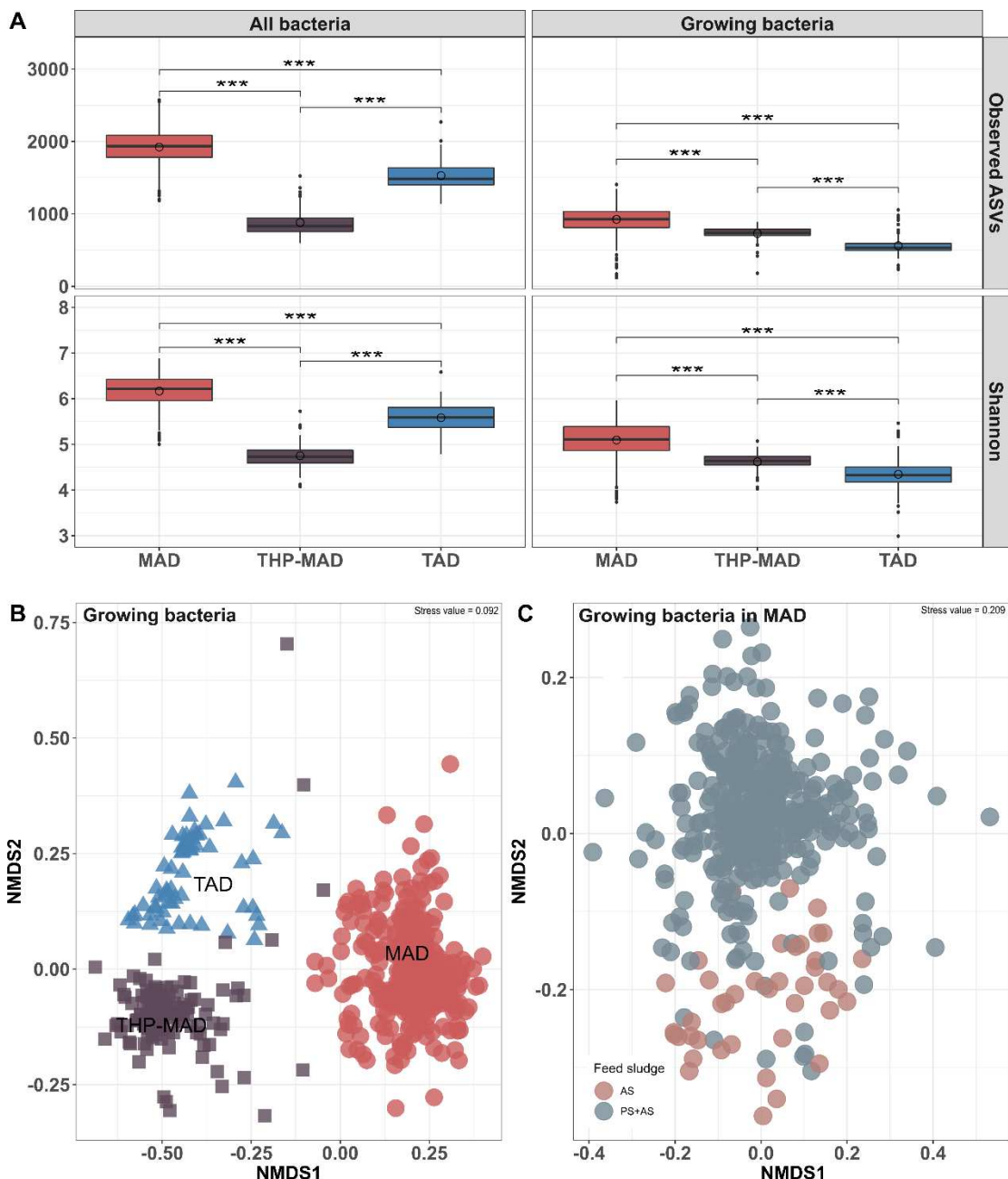
527

528 **Fig. 1 Composition of growing and non-growing ASVs in Danish ADs at WWTPs.**
529 The total ASVs (median relative abundance > 0.01%) divided into four groups based on
530 growth ratio (growing/non-growing) and relative abundance (high/low abundant, 0.1%
531 indicates the cutoff value). A and B show the composition of ASV counts and ASV
532 relative abundance for these four groups in MAD, THP-MAD, and TAD, respectively.
533 MAD = Mesophilic AD, THP = Mesophilic with thermal hydrolysis pretreatment, TAD
534 = Thermophilic AD.



535

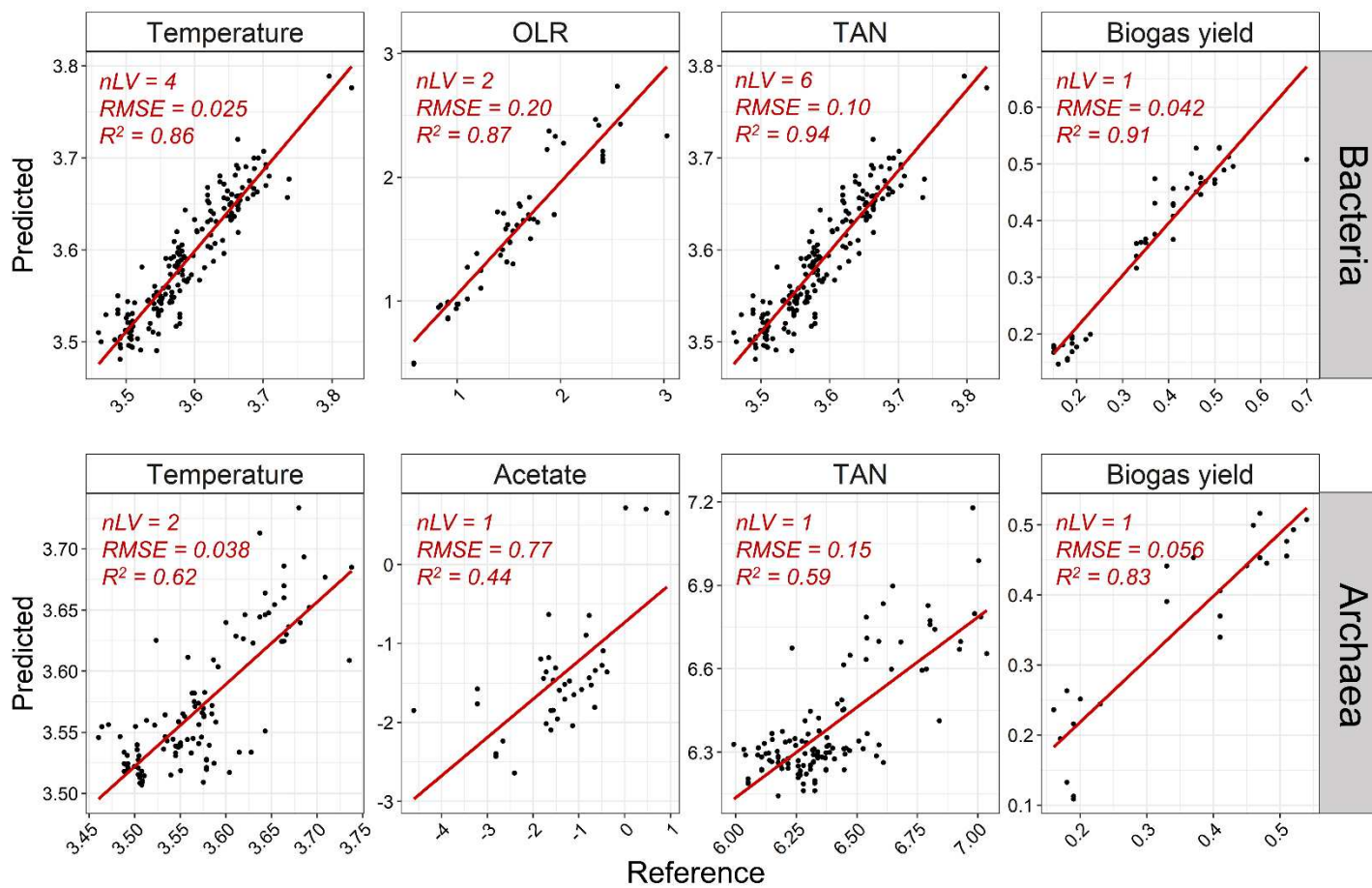
536 **Fig. 2 Boxplots of the most abundant species/ASVs in Danish ADs at WWTPs.** (A) The 25 most abundant bacterial species/ASVs in
537 MAD, (B) The 25 most abundant bacteria species/ASVs in TAD, (C) The 10 most abundant archaeal species/ASVs in MAD, (D) The 10
538 most abundant archaeal species/ASVs in TAD. The dots at the left in A and B indicate whether the species/ASVs are growing (ratio >10,
539 blue), non-growing or dying off (ratio <10, orange). MAD = Mesophilic AD, TAD = Thermophilic AD. Ratio refers to the digester to influent
540 relative read abundance ratio (please see **Additional file 3**). Sequences not possessing species-levels classification are shown here as
541 individual ASVs.



542

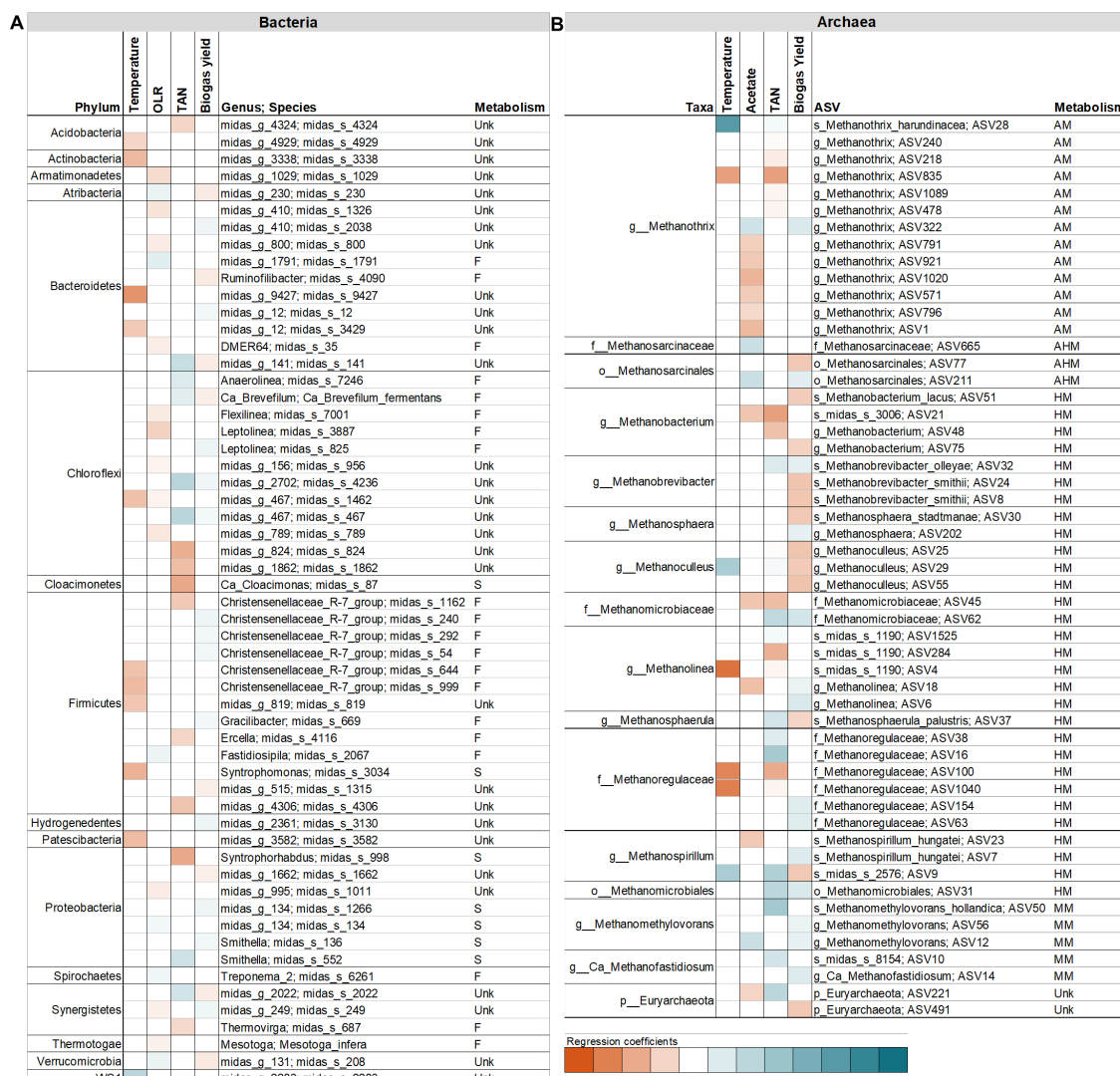
543 **Fig. 3 Alpha and beta diversity plots of bacterial and archaeal communities of three**
 544 **types of AD.** (A) Boxplots of observed ASVs and Shannon index of entire and growing

545 bacterial community, significant differences are indicated (Wilcoxon rank-sum test; ***,
 546 $p < 0.001$). (B) Non-metric multidimensional scaling (NMDS) plots of growing bacterial
 547 community structure based on weighted UniFrac matrix, (C) NMDS plots of growing
 548 bacterial community structure of MAD based on weighted UniFrac matrix. MAD =
 549 Mesophilic AD, THP-MAD = Mesophilic with thermal hydrolysis pretreatment process,
 550 TAD = Mesophilic AD, AS = Activated sludge, PS = Primary sludge.



551

552 **Fig. 4 Prediction plots of main drivers based on bacterial and archaeal microbiome in MAD by partial least squares regression.** MAD
 553 = mesophilic AD, OLR = organic loading rate, TAN = total ammonium nitrogen. nLV = number of selected components, RMSE = root mean
 554 squared error.



555

556 **Fig. 5 Partial least squares estimation for main driver for important growing**
557 **bacterial species (A) and archaeal ASVs (B) in MAD. $P < 0.05$, positive correlation in**
558 **blue, negative correlation in orange. F = Fermenters, S = Syntrophic bacteria, AM =**
559 **Acetoclastic methanogens, AHM = Acetoclastic or Hydrogenotrophic methanogens, HM**
560 **= Hydrogenotrophic methanogens, MM = Methylotrophic methanogens, Unk = Unknown.**

561 **Supplementary information**

562 **Additional file 1: Table S1.** Overview of WWTP digester capacities, type, and industrial load.

563 **Table S2.** Linear regression of key variables individually against alpha diversity using the
564 Shannon diversity index at MAD. **Table S3.** Permutational multivariate analysis (using
565 continuous variables only) of variance of beta diversity using weighted UniFrac matrix at MAD.

566 **Figure S1.** Comparison of classification between full-length exact sequence variants (FL-ESVs)
567 database and the SILVA_132_SSURef_Nr99 database on the top 50 ASVs in the digester sludge
568 samples from Danish wastewater treatment plants. **Figure S2.** Box plots of operational and
569 performance parameters of three types of AD. **Figure S3.** Spearman correlations on operational
570 and performance parameters in AD. **Figure S4.** Distribution of digester:feed relative read
571 abundance ratios for each ASV. **Figure S5.** (A) Relative abundance of the 20 most abundant
572 bacterial phyla in AD. (B) Relative abundance of the 50 most abundant bacterial genera in AD (n
573 = 564). **Figure S6.** Boxplots of the top 100 species/ASVs in MAD. **Figure S7.** Boxplots of the
574 top 100 species ASVs in TAD. **Figure S8.** Boxplots of the most abundant species/ASVs in THP-
575 MAD. **Figure S9.** Heatmap of the most abundant species/ASVs belonging to the genus T78 in
576 MiDAS 2 (split into the genera midas_g_156 and midas_g_467, all family Anaerolineaceae),
577 genus *Ca. Cloacimonas*, genus *Pelotomaculum*, midas_g_995, and genus *Methanothrix* in Danish
578 digesters at WWTPs. **Figure S10.** Relative abundance of the 25 most abundant archaeal genera
579 in AD (n = 402). **Figure S11.** Boxplots of alpha diversity measures of archaeal community of
580 three types of AD. **Figure S12.** Non-metric multidimensional scaling (NMDS) plots of bacterial
581 and archaeal community structure based on weighted Unifrac matrix colored by WWTPs. **Figure**
582 **S13.** Non-metric multidimensional scaling (NMDS) plots of all aacteria and archaea community
583 structures based on weighted Unifrac matrix. **Figure S14.** (A) Non-metric multidimensional
584 scaling (NMDS) plots of entire bacterial community structure based on weighted UniFrac matrix
585 in MAD. (B) Heatmap of 25 most abundant bacterial species in MAD digesters depending on the
586 composition of feed sludge (AS and PS). **Figure S15.** (A) Non-metric multidimensional scaling
587 (NMDS) plots of archaeal community structure based on weighted UniFrac matrix in MAD. (B)
588 Heatmap of 15 most abundant archaeal species in MAD digesters depending on the composition
589 of feed sludge (AS and PS). **Figure S16.** Prediction plots of other important parameters based on
590 bacterial and archaeal microbiome in MAD by partial least square regression. **Figure S17.**
591 Complete list for partial least squares estimation of key variables with growing bacterial species
592 (A) and archaeal ASVs (B) in MAD. **Figure S18.** Partial least squares estimation of key variables
593 with non-growing bacterial species in MAD.

594 **Additional file 2: Characterization of key parameters of anaerobic digestions**

595 **Additional file 3: Digester to influent relative read abundance ratios for each ASV**

596 **Acknowledgements**

597 We thank the operators at different WWTPs in Denmark for providing digester sludge
598 samples and plant records. The Chinese Scientific Research Council is acknowledged for
599 providing financial support to C. Jiang.

600 **Authors' contributions**

601 PHN and CJ conceived and designed the work. CJ, MP, and PHN wrote the manuscript.
602 CJ, MP, SK, and EY performed bioinformatic analysis, statistical analysis, and data
603 visualization. KSA and MSD provided bioinformatics support. MHA, MN, RHK, and LH
604 performed data collection, sampling, and lab procedures. JH and AAH contributed to
605 sample and plant record collection. CJ, MP, PHN, SK, MN, and MSD contributed to data
606 interpretation. All co-authors read and approved the final manuscript.

607 **Funding**

608 This research was funded by Innovation Fund Denmark [NomiGas, grant 1305-00018B]
609 and the Villum Foundation [Illumination of microbial dark matter, grant 13351].

610 **Availability of data and materials**

611 The raw amplicon sequences generated and analyzed during the current study were
612 uploaded to the NCBI Sequence Read Archive (SRA) data depository, with the project
613 number PRJNAXXXXX. Additional data can be shared upon request.

614 **Ethics approval and consent to participate**

615 Not applicable

616 **Consent for publication**

617 Not applicable

618 **Competing interests**

619 The authors declare that they have no competing interests

620 **Reference**

- 621 1. Nielsen PH. Microbial biotechnology and circular economy in wastewater treatment.
622 *Microb Biotechnol.* 2017;10:1102–5.
- 623 2. Puyol D, Batstone DJ, Hülsen T, Astals S, Peces M, Krömer JO. Resource Recovery
624 from Wastewater by Biological Technologies: Opportunities, Challenges, and
625 Prospects. *Front Microbiol. Frontiers*; 2017;7:2016.
- 626 3. Briones A, Raskin L. Diversity and dynamics of microbial communities in
627 engineered environments and their implications for process stability. *Curr Opin
628 Biotechnol.* 2003;14:270–6.
- 629 4. Ofițeru ID, Lunn M, Curtis TP, Wells GF, Criddle CS, Francis CA, et al. Combined
630 niche and neutral effects in a microbial wastewater treatment community. *PNAS.*
631 2010;107:15345–50.
- 632 5. Vanwonterghem I, Jensen PD, Dennis PG, Hugenholtz P, Rabaey K, Tyson GW.
633 Deterministic processes guide long-term synchronised population dynamics in
634 replicate anaerobic digesters. *ISME J.* 2014;8:2015–28.
- 635 6. Carballa M, Smits M, Etchebehere C, Boon N, Verstraete W. Correlations between
636 molecular and operational parameters in continuous lab-scale anaerobic reactors.
637 *Appl Microbiol Biotechnol.* 2011;89:303–14.
- 638 7. De Vrieze J, Saunders AM, He Y, Fang J, Nielsen PH, Verstraete W, et al. Ammonia
639 and temperature determine potential clustering in the anaerobic digestion
640 microbiome. *Water Res.* 2015;75:312–23.
- 641 8. Ho D, Jensen P, Batstone D. Effects of temperature and hydraulic retention time on
642 acetotrophic pathways and performance in high-rate sludge digestion. *Environ Sci
643 Technol.* 2014;48:6468–76.
- 644 9. Kim M, Ahn Y-H, Speece RE. Comparative process stability and efficiency of
645 anaerobic digestion; mesophilic vs. thermophilic. *Water Res.* 2002;36:4369–85.
- 646 10. Kirkegaard RH, McIlroy SJ, Kristensen JM, Nierychlo M, Karst SM, Dueholm MS,
647 et al. The impact of immigration on microbial community composition in full-scale
648 anaerobic digesters. *Sci Rep.* 2017;7:9343.
- 649 11. Lucas R, Kuchenbuch A, Fetzer I, Harms H, Kleinstreuber S. Long-term monitoring
650 reveals stable and remarkably similar microbial communities in parallel full-scale
651 biogas reactors digesting energy crops. *FEMS Microbiol Ecol.* 2015;91(3):fiv004.
- 652 12. Vanwonterghem I, Jensen PD, Rabaey K, Tyson GW. Temperature and solids
653 retention time control microbial population dynamics and volatile fatty acid
654 production in replicated anaerobic digesters. *Sci Rep.* 2015;5:8496.

655 13. Mei R, Nobu MK, Narihiro T, Kuroda K, Muñoz Sierra J, Wu Z, et al. Operation-
656 driven heterogeneity and overlooked feed-associated populations in global anaerobic
657 digester microbiome. *Water Res.* 2017;124:77–84.

658 14. Schnürer A, Nordberg Å. Ammonia, a selective agent for methane production by
659 syntrophic acetate oxidation at mesophilic temperature. *Water Sci Technol.*
660 2008;57:735–40.

661 15. Sundberg C, Al-Soud WA, Larsson M, Alm E, Yekta SS, Svensson BH, et al. 454
662 pyrosequencing analyses of bacterial and archaeal richness in 21 full-scale biogas
663 digesters. *FEMS Microbiol Ecol.* 2013;85:612–26.

664 16. Mei R, Kim J, Wilson FP, Bocher BTW, Liu W-T. Coupling growth kinetics
665 modeling with machine learning reveals microbial immigration impacts and
666 identifies key environmental parameters in a biological wastewater treatment
667 process. *Microbiome.* 2019;7:65.

668 17. Bocher BTW, Cherukuri K, Maki JS, Johnson M, Zitomer DH. Relating
669 methanogen community structure and anaerobic digester function. *Water Res.*
670 2015;70:425–35.

671 18. Morris R, Schauer-Gimenez A, Bhattad U, Kearney C, Struble CA, Zitomer D, et al.
672 Methyl coenzyme M reductase (mcrA) gene abundance correlates with activity
673 measurements of methanogenic H₂/CO₂-enriched anaerobic biomass. *Microb
674 Biotechnol.* 2014;7:77–84.

675 19. Tale VP, Maki JS, Struble CA, Zitomer DH. Methanogen community structure-
676 activity relationship and bioaugmentation of overloaded anaerobic digesters. *Water
677 Res.* 2011;45:5249–56.

678 20. Venkiteswaran K, Bocher B, Maki J, Zitomer D. Relating anaerobic digestion
679 microbial community and process function. *Microbiol Insights.* 2015;8:37–44.

680 21. Kucheryavskiy S. mdatools – R package for chemometrics. *Chemometr Intell Lab.*
681 2020;198:103937.

682 22. Callahan BJ, McMurdie PJ, Holmes SP. Exact sequence variants should replace
683 operational taxonomic units in marker-gene data analysis. *ISME J.* 2017;11:2639–43.

684 23. García-García N, Tamames J, Linz AM, Pedrós-Alió C, Puente-Sánchez F.
685 Microdiversity ensures the maintenance of functional microbial communities under
686 changing environmental conditions. *ISME J.* 2019;1–15.

687 24. Dueholm MS, Andersen KS, Petriglieri F, McIlroy SJ, Nierychlo M, Petersen JF, et
688 al. Comprehensive ecosystem-specific 16S rRNA gene databases with automated
689 taxonomy assignment (AutoTax) provide species-level resolution in microbial
690 ecology. *bioRxiv.* 2019;672873.

691 25. Nierychlo M, Andersen KS, Xu Y, Green N, Jiang C, Albertsen M, et al. MiDAS 3:
692 An ecosystem-specific reference database, taxonomy and knowledge platform for

693 activated sludge and anaerobic digesters reveals species-level microbiome
694 composition of activated sludge. *Water Res.* 2020;115955.

695 26. Quast C, Pruesse E, Yilmaz P, Gerken J, Schweer T, Yarza P, et al. The SILVA
696 ribosomal RNA gene database project: improved data processing and web-based
697 tools. *Nucleic Acids Res.* 2013;41:D590–6.

698 27. DeSantis TZ, Hugenholtz P, Larsen N, Rojas M, Brodie EL, Keller K, et al.
699 Greengenes, a Chimera-Checked 16S rRNA Gene Database and Workbench
700 Compatible with ARB. *Appl Environ Microbiol.* 2006;72:5069–72.

701 28. Cole JR, Wang Q, Fish JA, Chai B, McGarrell DM, Sun Y, et al. Ribosomal
702 Database Project: data and tools for high throughput rRNA analysis. *Nucleic Acids*
703 *Res.* 2014;42:D633–42.

704 29. Hao L, Michaelsen TY, Singleton CM, Dottorini G, Kirkegaard RH, Albertsen M, et
705 al. Novel syntrophic bacteria in full-scale anaerobic digesters revealed by genome-
706 centric metatranscriptomics. *ISME J.* 2020;1–13.

707 30. Kirkegaard RH, Dueholm MS, McIlroy SJ, Nierychlo M, Karst SM, Albertsen M, et
708 al. Genomic insights into members of the candidate phylum Hyd24-12 common in
709 mesophilic anaerobic digesters. *ISME J.* 2016;10:2352–64.

710 31. Lane DJ. 16S/23S rRNA sequencing. *Nucleic Acid Techniques in Bacterial*
711 *Systematics.* New York: Wiley; 1991. p. 125–175.

712 32. Muyzer G, Waal EC de, Uitterlinden AG. Profiling of complex microbial
713 populations by denaturing gradient gel electrophoresis analysis of polymerase chain
714 reaction-amplified genes coding for 16S rRNA. *Appl Environ Microbiol.*
715 1993;59:695–700.

716 33. Pinto AJ, Raskin L. PCR Biases Distort Bacterial and Archaeal Community
717 Structure in Pyrosequencing Datasets. *PLoS One.* 2012;7:e43093.

718 34. Albertsen M, Karst SM, Ziegler AS, Kirkegaard RH, Nielsen PH. Back to basics –
719 The influence of DNA extraction and primer choice on phylogenetic analysis of
720 activated sludge communities. *PLoS One.* 2015;10:e0132783.

721 35. Edgar RC. Search and clustering orders of magnitude faster than BLAST.
722 *Bioinformatics.* 2010;26:2460–1.

723 36. Edgar RC. UNOISE2: improved error-correction for Illumina 16S and ITS amplicon
724 sequencing. *bioRxiv.* 2016;081257.

725 37. Edgar RC. Accuracy of taxonomy prediction for 16S rRNA and fungal ITS
726 sequences. *PeerJ.* 2018;6:e4652.

727 38. R Core Team. R: A language and environment for statistical computing. R
728 Foundation for StatisticalComputing, Vienna, Austria.; 2019.

729 39. Wickham H. *ggplot2: Elegant Graphics for Data Analysis*. Springer-Verlag New
730 York; 2016.

731 40. Bastian M, Heymann S, Jacomy M. *Gephi: An Open Source Software for Exploring*
732 *and Manipulating Networks*. Third International AAAI Conference on Weblogs and
733 Social Media. 2009.

734 41. Caporaso JG, Kuczynski J, Stombaugh J, Bittinger K, Bushman FD, Costello EK, et
735 al. QIIME allows analysis of high-throughput community sequencing data. *Nat*
736 *Methods*. 2010;7:335–6.

737 42. Martens H, Martens M. Modified Jack-knife estimation of parameter uncertainty in
738 bilinear modelling by partial least squares regression (PLSR). *Food Qual Prefer*.
739 2000;11:5–16.

740 43. Calusinska M, Goux X, Fossépré M, Muller EEL, Wilmes P, Delfosse P. A year of
741 monitoring 20 mesophilic full-scale bioreactors reveals the existence of stable but
742 different core microbiomes in bio-waste and wastewater anaerobic digestion systems.
743 *Biotechnol Biofuels*. 2018;11:196.

744 44. Mata-Alvarez J, Dosta J, Romero-Güiza MS, Fonoll X, Peces M, Astals S. A critical
745 review on anaerobic co-digestion achievements between 2010 and 2013. *Renew*
746 *Sustain Energy Rev*. 2014;36:412–27.

747 45. Martí-Herrero J, Soria-Castellón G, Diaz-de-Basurto A, Alvarez R, Chemisana D.
748 Biogas from a full scale digester operated in psychrophilic conditions and fed only
749 with fruit and vegetable waste. *Renew Energy*. 2019;133:676–84.

750 46. Fotidis IA, Wang H, Fiedel NR, Luo G, Karakashev DB, Angelidaki I.
751 Bioaugmentation as a solution to increase methane production from an ammonia-rich
752 substrate. *Environ Sci Technol*. 2014;48:7669–76.

753 47. Luo G, Fotidis IA, Angelidaki I. Comparative analysis of taxonomic, functional, and
754 metabolic patterns of microbiomes from 14 full-scale biogas reactors by
755 metagenomic sequencing and radioisotopic analysis. *Biotechnol Biofuels*. 2016;9:51.

756 48. Chen Y, Cheng JJ, Creamer KS. Inhibition of anaerobic digestion process: A
757 review. *Bioresour Technol*. 2008;99:4044–64.

758 49. Tsapekos P, Kougias PG, Treu L, Campanaro S, Angelidaki I. Process performance
759 and comparative metagenomic analysis during co-digestion of manure and
760 lignocellulosic biomass for biogas production. *Appl Energy*. 2017;185:126–35.

761 50. Petriglieri F, Nierychlo M, Nielsen PH, McIlroy SJ. In situ visualisation of the
762 abundant Chloroflexi populations in full-scale anaerobic digesters and the fate of
763 immigrating species. Nerenberg R, editor. *PLoS One*. 2018;13:e0206255.

764 51. Lee J, Kim E, Han G, Tongco JV, Shin SG, Hwang S. Microbial communities
765 underpinning mesophilic anaerobic digesters treating food wastewater or sewage
766 sludge: A full-scale study. *Bioresour Technol*. 2018;259:388–97.

767 52. Lee S-H, Kang H-J, Haeng Lee Y, Jun Lee T, Han K, Choi Y, et al. Monitoring
768 bacterial community structure and variability in time scale in full-scale anaerobic
769 digesters. *J Environ Monit.* 2012;14:1893–905.

770 53. Nelson MC, Morrison M, Yu Z. A meta-analysis of the microbial diversity observed
771 in anaerobic digesters. *Bioresour Technol.* 2011;102:3730–9.

772 54. Rivière D, Desvignes V, Pelletier E, Chaussonnerie S, Guermazi S, Weissenbach J,
773 et al. Towards the definition of a core of microorganisms involved in anaerobic
774 digestion of sludge. *ISME J.* 2009;3:700–14.

775 55. Stokholm-Bjerregaard M, McIlroy SJ, Nierychlo M, Karst SM, Albertsen M,
776 Nielsen PH. A critical assessment of the microorganisms proposed to be important to
777 enhanced biological phosphorus removal in full-scale wastewater treatment systems.
778 *Front Microbiol.* 2017;8:718.

779 56. McIlroy SJ, Kristiansen R, Albertsen M, Karst SM, Rossetti S, Nielsen JL, et al.
780 Metabolic model for the filamentous ‘*Candidatus Microthrix parvicella*’ based on
781 genomic and metagenomic analyses. *ISME J.* 2013;7:1161–72.

782 57. Pelletier E, Kreimeyer A, Bocs S, Rouy Z, Gyapay G, Chouari R, et al. “*Candidatus
783 Cloacamonas Acidaminovorans*”: Genome Sequence Reconstruction Provides a First
784 Glimpse of a New Bacterial Division. *J Bacteriol.* 2008;190:2572–9.

785 58. McIlroy SJ, Kirkegaard RH, McIlroy B, Nierychlo M, Kristensen JM, Karst SM, et
786 al. MiDAS 2.0: an ecosystem-specific taxonomy and online database for the
787 organisms of wastewater treatment systems expanded for anaerobic digester groups.
788 Database. 2017;2017:bax016.

789 59. Leclerc M, Delgènes J-P, Godon J-J. Diversity of the archaeal community in 44
790 anaerobic digesters as determined by single strand conformation polymorphism
791 analysis and 16S rDNA sequencing. *Environ Microbiol.* 2004;6:809–19.

792 60. Hori T, Haruta S, Ueno Y, Ishii M, Igarashi Y. Dynamic Transition of a
793 Methanogenic Population in Response to the Concentration of Volatile Fatty Acids
794 in a Thermophilic Anaerobic Digester. *Appl Environ Microbiol.* 2006;72:1623–30.

795 61. Choi J-M, Han S-K, Lee C-Y. Enhancement of methane production in anaerobic
796 digestion of sewage sludge by thermal hydrolysis pretreatment. *Bioresour Technol.*
797 2018;259:207–13.

798 62. Wandera SM, Westerholm M, Qiao W, Yin D, Jiang M, Dong R. The correlation of
799 methanogenic communities’ dynamics and process performance of anaerobic
800 digestion of thermal hydrolyzed sludge at short hydraulic retention times. *Bioresour
801 Technol.* 2019;272:180–7.

802 63. Karakashev D, Batstone DJ, Angelidaki I. Influence of environmental conditions on
803 methanogenic compositions in anaerobic biogas reactors. *Appl Environ Microbiol.*
804 2005;71:331–8.

805 64. Levén L, Eriksson ARB, Schnürer A. Effect of process temperature on bacterial and
806 archaeal communities in two methanogenic bioreactors treating organic household
807 waste. *FEMS Microbiol Ecol.* 2007;59:683–93.

808 65. Li Y-F, Nelson MC, Chen P-H, Graf J, Li Y, Yu Z. Comparison of the microbial
809 communities in solid-state anaerobic digestion (SS-AD) reactors operated at
810 mesophilic and thermophilic temperatures. *Appl Microbiol Biotechnol.*
811 2015;99:969–80.

812 66. Goux X, Calusinska M, Lemaigre S, Marynowska M, Klocke M, Udelhoven T, et al.
813 Microbial community dynamics in replicate anaerobic digesters exposed sequentially
814 to increasing organic loading rate, acidosis, and process recovery. *Biotechnol
815 Biofuels.* 2015;8:122.

816 67. Xu R, Yang Z-H, Zheng Y, Liu J-B, Xiong W-P, Zhang Y-R, et al. Organic loading
817 rate and hydraulic retention time shape distinct ecological networks of anaerobic
818 digestion related microbiome. *Bioresour Technol.* 2018;262:184–93.

819 68. Razaviarani V, Buchanan ID. Reactor performance and microbial community
820 dynamics during anaerobic co-digestion of municipal wastewater sludge with
821 restaurant grease waste at steady state and overloading stages. *Bioresour Technol.*
822 2014;172:232–40.

823 69. Gou C, Yang Z, Huang J, Wang H, Xu H, Wang L. Effects of temperature and
824 organic loading rate on the performance and microbial community of anaerobic co-
825 digestion of waste activated sludge and food waste. *Chemosphere.* 2014;105:146–51.

826 70. Vanwonterghem I, Jensen PD, Ho DP, Batstone DJ, Tyson GW. Linking microbial
827 community structure, interactions and function in anaerobic digesters using new
828 molecular techniques. *Curr Opin Biotechnol.* 2014;27:55–64.

829 71. Pece M, Astals S, Jensen PD, Clarke WP. Deterministic mechanisms define the
830 long-term anaerobic digestion microbiome and its functionality regardless of the
831 initial microbial community. *Water Res.* 2018;141:366–76.

832 72. McIlroy SJ, Kirkegaard RH, Dueholm MS, Fernando E, Karst SM, Albertsen M, et
833 al. Culture-Independent Analyses Reveal Novel Anaerolineaceae as Abundant
834 Primary Fermenters in Anaerobic Digesters Treating Waste Activated Sludge. *Front
835 Microbiol.* 2017;8:1134.

836 73. Hao L, Bize A, Conteau D, Chapleur O, Courtois S, Kroff P, et al. New insights into
837 the key microbial phylotypes of anaerobic sludge digesters under different
838 operational conditions. *Water Res.* 2016;102:158–69.

839 74. Ariesyady H, Ito T, Okabe S. Functional bacterial and archaeal community
840 structures of major trophic groups in a full-scale anaerobic sludge digester. *Water
841 Res.* 2007;41:1554–68.

842 75. Ariesyady HD, Ito T, Yoshiguchi K, Okabe S. Phylogenetic and functional diversity
843 of propionate-oxidizing bacteria in an anaerobic digester sludge. *Appl Microbiol*
844 *Biotechnol.* 2007;75:673–83.

845 76. Narihiro T, Nobu MK, Kim N-K, Kamagata Y, Liu W-T. The nexus of syntrophy-
846 associated microbiota in anaerobic digestion revealed by long-term enrichment and
847 community survey. *Environ Microbiol.* 2015;17:1707–20.

848 77. Kristiansen R, Nguyen HTT, Saunders AM, Nielsen JL, Wimmer R, Le VQ, et al. A
849 metabolic model for members of the genus *Tetrasphaera* involved in enhanced
850 biological phosphorus removal. *ISME J.* 2013;7:543–54.

851 78. Jetten MSM, Stams AJM, Zehnder AJB. Methanogenesis from acetate: a
852 comparison of the acetate metabolism in *Methanothrix soehngenii* and
853 *Methanosarcina* spp. *FEMS Microbiol Rev.* 1992;8:181–97.

854 79. Gehring T, Niedermayr A, Berzio S, Immenhauser A, Wichern M, Lübken M.
855 Determination of the fractions of syntrophically oxidized acetate in a mesophilic
856 methanogenic reactor through an ¹²C and ¹³C isotope-based kinetic model. *Water*
857 *Res.* 2016;102:362–73.

858 80. Capson-Tojo G, Moscoviz R, Astals S, Robles Á, Steyer J-P. Unraveling the
859 literature chaos around free ammonia inhibition in anaerobic digestion. *Renew*
860 *Sustain Energy Rev.* 2020;117:109487.